

This discussion paper is/has been under review for the journal Natural Hazards and Earth System Sciences (NHESS). Please refer to the corresponding final paper in NHESS if available.

Investigation of the influence of topographic irregularities and two dimensional effects on the intensity of surface ground motion with one- and two-dimensional analyses

L. Yılmazoğlu¹ and G. Ç. İnce²

¹Postgraduate Student, Aksaray University, Division of Civil Engineering, Department of Geotechnical Engineering, 68100 Aksaray, Turkey

²Division of Civil Engineering, Department of Geotechnical Engineering, Faculty of Engineering, Aksaray University, 68100 Aksaray, Turkey

Received: 24 October 2013 – Accepted: 11 November 2013 – Published: 6 December 2013

Correspondence to: G. C. Ince (gokcecicekince@gmail.com)

Published by Copernicus Publications on behalf of the European Geosciences Union.



Title Page

Abstract

Introduction

Conclusions

Figures

14

1

1

1

Back

Close

Full Screen / Esc

[Printer-friendly Version](#)

Interactive Discussion

Abstract

In this work, the surface ground motion that occurs during an earthquake in ground sections having different topographic forms has been examined with one and two dynamic site response analyses. One-dimensional analyses were undertaken using the Equivalent-Linear Earthquake Response Analysis program based on the equivalent linear analysis principle and the Deepsoil program which is able to make both equivalent linear and nonlinear analyses and two-dimensional analyses using the Plaxis software. The viscous damping parameters used in the dynamic site response analyses undertaken with the Plaxis software were obtained using the DeepSoil program. In the dynamic site response analyses, the synthetic acceleration over a 475 yr replication period representing the earthquakes in Istanbul was used as the basis of the bedrock ground motion. The peak ground acceleration obtained different depths of soils and acceleration spectrum values have been compared. The surface topography and layer boundaries in the 5-5' section were selected in order to examine the effect of the land topography and layer boundaries on the analysis results were flattened and compared with the actual status. The analysis results showed that the characteristics of the surface ground motion changes in relation to the varying local soil conditions and land topography.

1 Introduction

The damage to structures during an earthquake is not only related to the superstructure. Although the earthquake-resistance of structures is important there are two significant factors; the earthquake characteristics and local soil conditions. The characteristics of earthquake waves may change while passing through the soils and the earthquake forces that impact on the structures situated on the ground surface may increase. Likewise, the earthquake waves may change the characteristics of the ground surface while passing through the soil. Local soil conditions have a significantly effect

Title Page	
Abstract	Introduction
Conclusions	References
Tables	Figures
◀	▶
◀	▶
Back	Close
Full Screen / Esc	
Printer-friendly Version	
Interactive Discussion	

the amplitude and frequency features thus the inertia forces of the ground acceleration have an effect on structures during an earthquake. Therefore, the behavior of the layers which constitute the foundation of the soil should be examined before the construction of structures.

5 Determining the behavior of soil layers during an earthquake is one of the important
problems encountered in earthquake engineering. The increase in the amplitudes of
the earthquake waves while passing through the soil layers close to the surface is
defined as soil amplification. The significant factors which affect ground amplification
10 include the dynamic characteristics such as; bedrock depth, thickness and types of
soil layers on bedrock, shear modulus and damping ratio, and local effects such as
variation of these characteristics by depth and deformation, lateral irregularities of soil
layers and topographic characteristics (Hasal, 2009).

The shear strength of a ground element that is under the influence of repeated stresses resulting from earthquake forces can be defined in two ways and in two stages.

15 The first definition refers to dynamic shear strength and it is considered to be the value of the repeated stress amplitude that causes unit deformation amplitudes that rapidly increase or exceed a definite limit value. The second definition is related to the static shear strength which is found as a result of the repeated stress. The general result from work in the literature is that the shear stresses from higher magnitude earthquakes 20 may give rise to major deformations and landslides. Another result is that the major deformations arising from the repeated stress applications may cause softening and the effective stresses are decreased through the increase of pore water pressure and thus, the shear strength is reduced (Ansai et al., 1995).

25 The calculation methods developed for the dynamic analysis of soils are generally defined in terms of one, two or three dimensions depending on the requirement of the problem to be resolved. Since for the two and three dimensional analyses two or three dimensional geometry of layers in the ground sections are required, the one-dimensional approach is often preferred. However, in the one-dimensional dynamic analysis of soils; the surface topography, slope of layers and the effect of the limited

L. Yılmazoğlu and
G. Ç. İnce

Title Page

tract

Introduction

Conclusion

References

Conclusions References

References

Tables

Figures

1

1

Close

Full Screen / Esc

Printer friendly Version

Interactive Discussion

width of layers are ignored. The fact that the soils horizontally have a limited width causes the wave motion transformations in the valley edges, thus the frequency content of the ground motion and its effect on the surface may change from the middle of valleys towards edges. However, the effects of the second and even the third dimension emerge in narrow valleys, edges of wide valleys and hillsides (Kale, 2008).

2 Geology and topography of the region

This work was undertaken within the area known as the historical peninsula of Istanbul as shown in Fig. 1.

2.1 Geology

10 The geological map (Fig. 1) and selected sections used in this work were derived from a previous scientific study (Ince et al., 2008) in which geological surveys were carried out in and around the investigation field and from the work undertaken in which they obtained data from 125 shallow and deep drillings and investigation trenches in the area. Figure 1 shows two distinct outcropping formations in the study area that are

15 covered with layers of alluvium and artificial fill. The older of the two formations is the Lower Carboniferous Trakya formation, which constitutes the bedrock in the area and is composed of interbedded sandstone (graywacke), siltstone and claystone. The other group comprises units seated unconformably on the Trakya formation and consists of

20 Upper Oligocene – Upper Miocene deposits composed of interbedded sand, clay and carbonates. The Upper Oligocene – Upper Miocene deposits cover extensive areas both within the study area and in other parts of the European side of Istanbul. These deposits start in depositional sequence with interbedded clay and sand, later continuing with intercalations of gravelly sand, and, in the upper levels, interbedded marl and limestone due to increased carbonate content (as seen in the Gürpınar, Çukurçeşme, Gündöken, Bakırköy, Belgrad formations) (Yıldırım and Savaşkan, 2003).

[Title Page](#)

[Abstract](#)

[Introduction](#)

[Conclusions](#)

[References](#)

[Tables](#)

[Figures](#)

◀

▶

◀

▶

[Back](#)

[Close](#)

[Full Screen / Esc](#)

[Printer-friendly Version](#)

[Interactive Discussion](#)

2.2 Topography

The peninsula which constitutes the investigation field is bounded by the Golden Horn in the north, the Istanbul Bosphorus in the east and the Sea of Marmara in the south. This peninsula consists of three ridges. The Edirnekapi-Fatih-Beyazıt and

5 Topkapı-Aksaray ridges lie in a northeast-southeast direction and are separated by the Yenibahçe stream bed (Vatan Avenue). The highest part of Edirnekapi-Fatih-Beyazıt ridge reaches +75 m around Edirne and the ridge of Topkapı-Aksaray is +55 m high. The third ridge is Sarayburnu-Sultan Ahmet that lies in a northeast-southwest direction reaching a height of +45 m near Sarayburnu. Upright topography is observed in the
10 places where the greywacke rocks belonging to the Trakya Formation are located, the broad and almost-horizontal ridge plains are found where Bakırköy formation marl limestone is situated this is due to the partial resistance of the formation against abrasion and the slopes increase where Gürpınar formation, composed of green clays, surfaces.
15 The arcview program was used to produce a three-dimensional image of the study area using height data at intervals of 50 m (Fig. 2).

2.3 The analysed cross sections

As shown in Fig. 1 the study area was divided into 5 cross sections which are detailed below.

20 2.3.1 Section 1-1'

This is the smallest section, about 2500 m long in a northeast-southwest direction, situated between the quarters of Eminönü-Kumkapı located in the farthest east part of the section. The section consists of bedrock which is greywacke at the bottom. There are coastal sediments with a thickness of 40 m in the sea of the Golden Horn to the
25 north. The artificial layers of fill with a thickness of 40 m in the sea are adjacent to the

Topographic irregularities and 2-D effects on the surface

L. Yılmazoğlu and
G. Ç. İnce

[Title Page](#)

[Abstract](#)

[Introduction](#)

[Conclusions](#)

[References](#)

[Tables](#)

[Figures](#)

◀

▶

◀

▶

[Back](#)

[Close](#)

[Full Screen / Esc](#)

[Printer-friendly Version](#)

[Interactive Discussion](#)

Topographic irregularities and 2-D effects on the surface

L. Yılmazoğlu and
G. Ç. İnce

[Title Page](#)

[Abstract](#) [Introduction](#)

[Conclusions](#) [References](#)

[Tables](#) [Figures](#)

◀

▶

◀

▶

[Back](#) [Close](#)

[Full Screen / Esc](#)

[Printer-friendly Version](#)

[Interactive Discussion](#)



estuary (Golden Horn) sediments. There are clayey levels of the Gürpınar formation reaching a thickness of 80 m in the middle of the section and partly including layers of sand. There are alluvial sediments with a thickness of 10 m on the coastline in the south. The top layer is fully covered with artificial layers of fill. These fills are generally composed of construction waste or marble fragments. Figure 3, shows section 1-1' with the points 1A, 1B, 1C, 1D, 1E and 1F where the analyses were undertaken.

2.3.2 Section 2-2'

This section runs from the east of the Unkapanı Bridge in the north to Yenikapı in the south a distance of approximately 2820 m. The greywacke called Lower Carboniferous old and the Trakya formation forming the bedrock of the region and consisting of grey, brown, multi-crackled, thin-medium layered sandstones, siltstones, clay stones and shale are quite close to the surface in this section and have even partly surfaced. The artificial fills in the coastal region to the north and south reaching a thickness of 30–40 m in the sea. In the middle of the section, the artificial fill thickness from bedrock to surface is 10 m. The stack called the Gürpınar formation sits discordantly on the Trakya Formation, it is composed of plentiful fissures, excessively consolidated clays, clay stones and sand lenses of a maximum 50 m thickness. The Bakırköy formation of forming the upper levels of the Gürpınar formation is about 20 m underneath the artificial fills on hilly plains in the section. In Fig. 4, section 2-2' is shown with the 2A, 2B, 2C, 2D, 2E and 2F points where the analyses were made.

2.3.3 Section 3-3'

This section has a length of 3840 m and intersects with the ridges of Edirnekapı-Fatih-Beyazıt and Topkapı-Aksaray and the Yenibahçe stream bed (Vatan Avenue) where the slopes end and flat areas begin at the lower levels. There are estuary coastal sediments in the sea in the north and alluvial sediments in the south. The clays of the Gürpınar formation thickness sitting on the bedrock greywacke discordantly are about 60–70 m

2.3.4 Section 4-4'

5 This section with a length of approximately 4920 m is in the farthest west part of the investigation area. In this section which has thick clayey levels, the thickness of Gürpinar Formation reaches 140 m. As in section 3-3', the high places of Edirnekapi-Fatih-Beyazit and Topkapı-Aksaray ridges and the high levels of Yenibahçe stream bed are located in this section. The limestone levels of the Bakırköy formation with 10 a thickness of 30–35 m are placed in the upper levels of Gürpi nar formation in the west of the section. The artificial fill is about 5–10 m thick in the top levels. In Fig. 6, section 4-4' is shown with the points of 4A, 4B, 4C, 4D, 4E, 4F, 4G, 4H, 4I, 4J and 4K where the analyses were made.

2.3.5 Section 5-5'

15 This section is the longest at about 5580 m. It lies in an east-west direction and ends in Sarayburnu to the west and Zeytinburnu in the east. The bedrock surfaces just underneath the greywacke artificial fill on the hilly plains where the Topkapı Palace is situated. The Gürpınar formation thickness lies at approximately 140 m on the bedrock in the east of the section and the Bakırköy formation on this stack is 25 m. The thickness
20 of the Gürpınar formation within the borders of Eminönü in the west of the section is about 50–60 m. The Bakırköy formation is just visible seen in this section. The fill layers situated at the top levels are 30 m deep in the valley. In Fig. 7, section 5-5' is shown with the points of 5A, 5B, 5C, 5D, 5E, 5F, 5G, 5H, 5I, 5J and 5K where the analyses were made.

Title Page

Abstract

Introduction

Conclusions

Figures

1

1

Back

Close

Full Screen / Esc

[Printer-friendly Version](#)

Interactive Discussion



3 One- and two-dimensional analyses

3.1 One-dimensional analysis

When a fault line cracks below the ground surface, object waves are emitted from the source in all directions and when they reach the borders of different geologic units 5 they are reflected and refracted. Since the transmission speed of the wave units in the shallow depth is slower than deeper ones, the inclined beams colliding with the layer boundary are generally refracted towards a more vertical position. The refractions that occur until the beam reaches the ground surface cause them to be refracted mostly in a direction close to the vertical. One-dimensional ground reaction analyses are based 10 on the assumption that all the borders are horizontal and that the ground reaction generally results from the waves (SH waves) emitted from the bedrock vertically. In the one-dimensional ground reaction analysis, the ground and bedrock surfaces are considered to have an infinite horizontal extent.

In this study, one-dimensional analyses were carried out at the following four points; 15 heel, skirt and top of the hillside together with the hilly plain. These points were selected in accordance with the Equivalent-Linear Earthquake Response Analysis (EERA) and DeepSoil computer programs, the field topography and formations (Table 1). EERA (Bardet et al., 2000) is a computer program prepared in Excel according to the content 20 of Shake (Schnabel et al., 1972), which is a computer program that is widely used in geotechnical earthquake engineering. In this analysis method, it is accepted that the non-linear behaviors of grounds can be approximately represented by the damped linear elastic model. However, the stress-deformation characteristics of the ground are defined by the shear modulus (G) and equivalent damping ratios (D) changing by unit deformation level (γ). The behavior is accepted as resulting from the shear wave 25 emitting vertically from the bedrock to the surface. The fact that the shear modulus and damping depend on deformation is considered with an equivalent linear method based on the average effective unit deformations calculated for each layer. The G/G_{\max} and damping relations depending on deformation and belonging to all formations is used

[Title Page](#)

[Abstract](#)

[Introduction](#)

[Conclusions](#)

[References](#)

[Tables](#)

[Figures](#)

◀

▶

◀

▶

[Back](#)

[Close](#)

[Full Screen / Esc](#)

[Printer-friendly Version](#)

[Interactive Discussion](#)

in EERA are collectively shown in Figs. 8 and 9. Also, the minimum and maximum values of the unit volume weight, material type and shear wave speeds belonging to the formations are given in the Table 2.

The Deepsoil program undertakes analyses in both frequency and time. It can make both linear and equivalent analyses concerning frequency, and both linear and nonlinear analyses concerning time. In this study; equivalent linear and nonlinear analysis methods were used for the Deepsoil analyses. In the nonlinear analysis producing analyses in the area of time, the layer thicknesses have been adjusted based on the maximum frequency and in the $h = Vs/4f_{\max}$ formula, the analysis was carried out by choosing a layer so that f_{\max} will be between 25 and 50 Hz (Hashash et al., 2009). The material characteristics of each layer shown in Figs. 8 and 9 were entered and compared with the characteristics of the reference material, then, when two graphs gave the approximate results, the next step was begun. The earthquake record used in the next stage was produced by the TARSCTHS (Papageorgiou et al., 2000) program in accordance with the NEHRP acceleration behavior spectrum based on the spectral acceleration value that would arise in the bedrock artificially. In the next and final stage where dominant frequencies/modes were determined for the nonlinear analysis, the graphs were compared in order to ensure the analysis in the field of frequency was in accord with the field of time. In the case of the values in the graph were not close to each other, the 1st and 2nd mode values were changed and the transactions were repeated and alignment was been achieved between the two graphs. As specified in the manual version of the Deepsoil program, the concordant graphs of the values 1 and 8 gives as "Default" for the 1st and 2nd modes were provided in most of the analyses and the 1st and 2nd mode values found in this way were substituted in Eq. (1) and Rayleigh α and Rayleigh β values were calculated.

$$\alpha = 2\xi \frac{w_i w_j}{w_i + w_j} \quad \beta = 2\xi \frac{1}{w_i + w_j} \quad (1)$$

Here, ξ ; represents the equivalent damping ratio, w_i and w_j represent the angular frequency values in the i and j modes. The results can be obtained as graphs

Topographic irregularities and 2-D effects on the surface

L. Yılmazoğlu and
G. Ç. İnce

[Title Page](#)

[Abstract](#)

[Introduction](#)

[Conclusions](#)

[References](#)

[Tables](#)

[Figures](#)

◀

▶

◀

▶

[Back](#)

[Close](#)

[Full Screen / Esc](#)

[Printer-friendly Version](#)

[Interactive Discussion](#)

for each layer including the acceleration-time, stress-time, deformation-time, stress-deformation, amplitude-frequency, and the peak spectral acceleration-period.

3.2 Two-dimensional analysis

One-dimensional ground response analysis methods are quite useful in flat or slightly inclined surfaces close to a material border. There are many cases of this kind in practice and one-dimensional analyses are widespread in geotechnical earthquake engineering practices. However, one-dimensional wave propagation assumption is not fit for purpose in many other problems encountered in practice. Therefore, two or maybe three-dimensional analyses are needed for all cases that involve rigid or embedded heavy structures or walls and tunnels on inclined or irregular surfaces. Problems in which one dimension is greater than the others can be mostly handled as a two-dimensional planar unit deformation problem. Two-dimensional analyses can be undertaken using finite element method which finds approximate results for mathematical problems encountered in many branches of engineering. This method is used in areas of ground-structure interaction, consolidation, stress-deformation, loading, bearing capacity, flow net and ground dynamics in civil engineering and in other cases of material variety.

In this study, the PLAXIS version software in conjunction with the finite element method in two-dimensional analyses was used. The version was developed for the applications of geotechnical engineering. In the analyses, problems are analyzed in a static manner and 2-dimensionally under axial symmetric geometrical conditions. In the program, the stress-deformation behavior of the material is modeled with nonlinear solution techniques. In this model, Poisson Ratio (ν), cohesion (c) internal friction angle (φ), expansion angle (ψ), dry and natural unit volume weights of the ground (γ_k and γ_n), horizontal and vertical permeability coefficients (k_v and k_h) and shear wave speed (V_s) are entered into the program. The elasticity modulus and shear modulus are automatically calculated by the program using these values. After defining the material parameters, the stage of forming a finite element net is started.

3.2.1 Material properties used in the analysis

The Plaxis program is capable of working with five different material models at the same time including Linear Elastic (LE), Mohr-Coulomb (MC), Jointed Rock (JR), Soft Soil (SS), Soft Soil Creep Model (SSC) and Hardening Soil Model (HS) in order to determine the ground properties. The Trakya formation in this study is bedrock was defined with the linear elastic material model, while the estuary coastal sediments were defined with the soft soil model. Alluvial, Çukurçeşme and Gürpınar formations were defined with the Mohr-Coulomb model and all the other formations were defined with the hardening soil material model. The other values belonging to the formations entered into the program are shown in Table 3.

The α and β damping parameters were obtained from Eq. (1) at the points where the analyses were to be made according to the angular frequency values of ω_1 and ω_2 which were obtained from Rayleigh damping curve produced from non-linear analysis in the Deepsoil program (Table 4).

3.2.2 Earthquake motion input file used in the analysis

The earthquake motion amplitudes entered into the two-dimensional dynamic analysis at the level of bedrock were synthetically produced with the TARSCTHS (Papageorgiou et al., 2000) program. The peak and spectral acceleration values of the bedrock used in the program were produced probabilistically using the source zoning carried out by Bosphorus University (İnce, 2012).

4 Analysis results and evaluations

One and two-dimensional analyses were made at the points where the field topography changed and on the hillside, the heel of hillside, hilly plains and coastal plains where the results were expected to differentiate and at the same time at the points where different formations are layered based on depth. The points chosen, their formation information

[Title Page](#)

[Abstract](#)

[Introduction](#)

[Conclusions](#)

[References](#)

[Tables](#)

[Figures](#)

◀

▶

◀

▶

[Back](#)

[Close](#)

[Full Screen / Esc](#)

[Printer-friendly Version](#)

[Interactive Discussion](#)

and topographical positions are shown in Table 1. The results of the analysis results were obtained as a peak acceleration change on the section surfaces and the section depth and also as spectral acceleration-period graphs for the selected points.

4.1 Change of peak ground acceleration values on the surface

5 In one-dimensional analyses the earthquake wave progresses only vertically upwards from the bedrock. However, it progresses in two dimensions in the direction of earthquake wave propagation from left to right. In this case, as the effect of the topographical change on the surface acceleration can be observed in the two-dimensional analysis, the effect of layer thicknesses appears in one dimension. In this 10 study, the results of one and two-dimensional analyses were evaluated with and within each other and the correlation between them was obtained.

For the one dimensional analysis, the EERA and DEEPSOIL (equivalent linear, EL, and nonlinear, NL) programs were used and the PLAXIS finite element program was used for the two-dimensional analyses. For all the sections, the change of the maximum 15 surface acceleration on the ground surface is shown together with the change of peak acceleration value belonging to the bedrock as shown in Figs. 10–14.

The results of the one-dimensional analysis show a descending tendency between points 1A and 1C where the fill layer that was 14 m at the beginning gave way to a thick clay layer reaching 40 m. In the two-dimensional analysis, an increase in the 20 acceleration value was observed upwards from the slope. Here, it could be thought that the changing topography appeared in the two-dimensional analysis.

The decrease in the clay layer of about 10 m between the points of 1B and 1D (between two peak points) gave way to an increase in the fill layer in almost the same amount. In this case, while the acceleration value increased in the one-dimensional 25 analyses, on the contrary it was observed that the acceleration value decreased in the two-dimensional analyses.

It is seen that the clay layer between the 1D peak point and the 1F point at sea level ends with faulting and the bedrock approaches to the surface. The thickness of

[Title Page](#)

[Abstract](#)

[Introduction](#)

[Conclusions](#)

[References](#)

[Tables](#)

[Figures](#)

◀

▶

[Back](#)

[Close](#)

[Full Screen / Esc](#)

[Printer-friendly Version](#)

[Interactive Discussion](#)

Topographic irregularities and 2-D effects on the surface

L. Yılmazoğlu and
G. Ç. İnce

[Title Page](#)

[Abstract](#) [Introduction](#)

[Conclusions](#) [References](#)

[Tables](#) [Figures](#)

◀

▶

◀

▶

[Back](#)

[Close](#)

[Full Screen / Esc](#)

[Printer-friendly Version](#)

[Interactive Discussion](#)

a thickness of 30 m at the 3B peak point. In this case, it is seen that the acceleration values increase in the one-dimensional analyses. With the decrease of the thickness of fill layer at the 3C point, the acceleration value increases and the clayey layer reaches a thickness of 30 m, as a result, the peak values are achieved.

5 The thickness of the clayey layer between the 3B and 3D points decreases until the valley and then increases again in the second hilly place but the effect of these changes is observed as a decrease in the acceleration graph. While the clayey layer with a thickness of 5 m between the 3D and 3H points which are the top levels of the second hill gradually decreases from the top down and gives way to a fill layer of 6 m
10 after ending with faulting. This change gives rise to an increase in the acceleration values. The fill layer between the 3H and 3G points ends and gives way to estuary sediments reaching a thickness of 45 m in the sea. In this case, it is seen that the acceleration values rapidly reduce and even fall below the acceleration value of the bedrock. It is observed that the estuary sediments located at the sea bottom in the
15 form of slurry that has the effect of decreasing the earthquake acceleration.

On the other hand, examining the two-dimensional acceleration graph shows that the acceleration value decreases until the 3E point located on the second hilly area and exhibits a behavior almost consistent with the one-dimensional analysis results after this point.

20 In Sect. 4, it is observed that the results of the one and two dimensional analyses are more compatible in comparison to the other sections. In the two-dimensional analysis, the beginning of the graph is just the opposite to the sections but as in accordance with the one-dimensional analyses. This difference that occurs at the beginning results from the calculations of the Plaxis program under the initial limit conditions. The values 25 between the 4E and 4D points where the field topographical incline increases from left to right sharply declines in each of the three graphs. It is thought that the parameter effective in the one-dimensional analysis is the Bakırköy limestone located at the upper levels of the section and gradually thickening. Between points 4D and 4C the surface topography and the thicknesses of Bakırköy limestone levels change and their effect is

L. Yılmazoğlu and
G. Ç. İnce

Title Page
Abstract Introduction
Inclusions References
Tables Figures
◀ ▶
◀ ▶
Back Close
Full Screen / Esc
Printer-friendly Version
Interactive Discussion

Topographic irregularities and 2-D effects on the surface

L. Yılmazoğlu and
G. Ç. İnce

[Title Page](#)

[Abstract](#) [Introduction](#)

[Conclusions](#) [References](#)

[Tables](#) [Figures](#)

◀

▶

◀

▶

Back

Close

[Full Screen / Esc](#)

[Printer-friendly Version](#)

[Interactive Discussion](#)

again observable in the results of the three analyses. However, the EERA results fall below the bedrock peak acceleration values until the 4B point, that is, the end of the Bakırköy formation. Between points 4B and 4A where the old stream bed is situated at the bottom of the valley and the alluvial layer is located, the values increase and reach a peak at the 4A point. After this point, while the wave moves upwards from the slope, the acceleration value decreases in all analyses and reaches the lowest levels on the hill. In the one and two dimensional analyses, different parameters can be said to have an effect on this change. The clayey levels which are quite thick might cause the acceleration to decrease in the one-dimensional analyses (from 20 m to 50 m). On the other hand, such a decrease is observed in all the sections in the two dimensional analyses when going upwards from slope. From point 4H at the peak of the section down to the 4I point, the acceleration value increases again in the one-dimensional analyses and the result of the two-dimensional analyses also increases, while the clayey layer decreases. The surface incline continues downwards from points 4I–4J at the same time, the bedding changes and clayey levels end and give way to the fill layer. The thickness of the fill layer gradually increases towards the coast. In this case, the values of the surface acceleration reach peak levels. At the 4K point where the estuary coastal sediments are situated, the values fall to the lowest levels. It is observed that the estuary coastal sediments located in the sea in the form of slurry effectively lower the acceleration value.

In Sect. 5, the initial values of Plaxis begin differently due to the limit conditions as in the other sections. It is observed that the thickness of the clayey layer rises to 73 m and the acceleration value decreases until the 5C point where the thickness of the Bakırköy limestone increases. From the 5C point on the hill down to the 5D point, which is located downwards from the slope, the thickness of the clayey layer decreases and falls to 20 m. The Bakırköy limestone located on the clayey layer gradually decreases and disappears. In this case, the acceleration value in the one-dimensional analyses increases. The bedrock between the 5D and 5E points at the bottom of the valley almost surfaces, and only a fill layer of 5 m remains on the bedrock. In this

case, the acceleration value in the one-dimensional analyses decreases however, on the contrary, the acceleration value in the two-dimensional analysis increases. The influential aspect here is thought to be the second dimension effect which occurs downwards from the hillside. Between the 5E point where the bedrock and the fill of 5 m are located upwards from the slope and the 5F point where a clayey layer of 5 m and fill of 5 m are placed on the bedrock, the acceleration value increases in the one-dimensional analyses and reaches a peak at 5F. On the contrary, in the two-dimensional analyses the acceleration value decreases. The field topography and changing upwards from the slope can be influential in the two-dimensional analyses.

5 The acceleration value falls to the lowest values between the 5F and 5H points in the one-dimensional analyses. The clayey layer that thickens (from 25 m to 38 m) and the limestone levels that are partly placed are thought to be influential here. Another important point is that the clayey levels up to 20–25 m increase the acceleration but decreases the acceleration after 25 m in the one-dimensional analyses. In the two-dimensional analyses, the acceleration value increases between the 5F and 5G points upwards from the slope and remains stable on the hill between the 5G and 5H points.

10 15

In the case where the clayey levels between 5H and 5I fall from 35 to 18 m, it is observed that the acceleration value increases in the one-dimensional analyses and reaches the peak level at 5I. However, a great change is not seen in the two-dimensional analyses moving downwards from the slope.

20 The thickness of the 15 m fill layer decreases to 5 m between points 5I and 5J (the bottom and peak points of the valley), in which case the acceleration value gradually decreases in the one-dimensional analyses. In the two-dimensional analyses, a decrease is seen in the acceleration going downwards from slope.

25 4.2 Change of peak ground acceleration values by depth

The results of the analyses made at the points selected along the borders of the changing layer are shown for all sections together with the one and two-dimensional analyses results in Figs. 15–19 in order to examine the change in the layer border.

Topographic irregularities and 2-D effects on the surface

L. Yılmazoğlu and
G. Ç. İnce

[Title Page](#)

[Abstract](#)

[Introduction](#)

[Conclusions](#)

[References](#)

[Tables](#)

[Figures](#)

◀

▶

[Back](#)

[Close](#)

[Full Screen / Esc](#)

[Printer-friendly Version](#)

[Interactive Discussion](#)

All the analysis results are in consistent in terms of the change-depth graph of the 1D point, the acceleration value rapidly increases from 0.2 to 0.45 especially after 20 m where the artificial fill layer starts. As the results at the 1B and 1F points are higher in the two-dimensional analyses, the lowest values are obtained from the EERA analysis in the one-dimensional analyses.

When examining the acceleration-spectrum graph strong spectral reactions ranging between 0.77–1.04 g at 1F, 0.97–1.35 g at 1B and 1.05–1.3 g at 1D are observed at each of three points in a short time interval of 0.10–0.40 s. The results obtained by PLAXIS is quite different and larger values were obtained compare with one dimensional analyses.

While the results of the two-dimensional analysis result changes from 0.19 to 0.27 at point 2A that is at the beginning of the slope, they rapidly increase to the values of 0.53–0.78 in the final 20 m where the bedrock disappears and the clayey layer appears. The prevailing interval of this point on the surface is 0.17–0.41 s. and the peak spectral acceleration values change from 2.02 to 2.19 in a short time interval. At the 2C point where the bedrock is quite close to the surface, the results of all the analyses are in accord and increase after 20 m. The prevailing time interval of the spectrum changes from 0.05 to 0.34 as the peak spectral acceleration value remains at 0.05 and instantly increases from 0.78 to 1.7 for the analyses and then the range is 0.6–0.8. The results obtained by PLAXIS is a similar at point 2A but quite different at point 2C.

At the 3B point which consists of a clayey layer of about 30 m and a fill layer of 5 m, the results of one-dimensional analyses continue in accordance with each other along the depth and rapidly increases from 0.27 to 0.6 at the final 20 m. The prevailing period value is from 0.11 to 0.49 and the peak spectral acceleration values range from 1.83 to 2.35. The value of two-dimensional analysis rises from 0.25 to 0.5 between 40 and 70 m and then remains stable throughout the clayey layer.

At the 3H point where the bedrock and an artificial fill layer of 3 m are situated, the results of the two-dimensional analyses are greater than those of the one-dimensional analysis but give the same values as the one-dimensional analysis with the initiation of

Topographic irregularities and 2-D effects on the surface

L. Yılmazoğlu and
G. Ç. İnce

[Title Page](#)

[Abstract](#) [Introduction](#)

[Conclusions](#) [References](#)

[Tables](#) [Figures](#)

◀

▶

◀

▶

[Back](#) [Close](#)

[Full Screen / Esc](#)

[Printer-friendly Version](#)

[Interactive Discussion](#)

Topographic irregularities and 2-D effects on the surface

L. Yılmazoğlu and
G. Ç. İnce

[Title Page](#)

[Abstract](#) [Introduction](#)

[Conclusions](#) [References](#)

[Tables](#) [Figures](#)

◀

▶

◀

▶

[Back](#)

[Close](#)

[Full Screen / Esc](#)

[Printer-friendly Version](#)

[Interactive Discussion](#)

the fill layer. The one-dimensional analysis results continue very close to each other and rapidly increases from 0.22–0.29 to 0.54–0.67 after the final 10 m. The peak spectral acceleration values of 1.87–2.37 g are achieved in a short time interval of 0.20–0.30 s. Three times the difference between the results of the one and two dimensional analyses is observed.

In the depth-acceleration graph of the 4E point where the fill layer has a thickness of 65 m, the Bakırköy limestone of 3 m and a fill layer of 6 m on the top, the results of the one-dimensional analyses continue in accordance with each other and rapidly increase from 0.23–0.28 to 0.41–0.57 especially after the final 10 m the two-dimensional analysis results give greater values. The peak spectral acceleration increases to values 1.46–1.63 for 0.15 s. as the prevailing time interval is 0.13–0.37.

The 4A point situated at the bottom of the valley consists of a clayey layer of 25 m and a fill layer of 3 m. The results of the one-dimensional analyses are in accordance and increase from 0.25 to 0.33 to a value of 0.55 after the final 10 m. The result of the two dimensional analysis is greater and discordant compared to that of the one-dimensional analysis and exhibits a zigzag behavior. It can be seen that there are two prevailing peak points in the spectral acceleration graph. The peak spectral acceleration value changes from 1.28 to 1.52 values within 0.25 s.

The 4H point situated on a hill which consists of 45 m clay and 2 m fill. While the EERA value is lower in the one-dimensional analyses, the acceleration value increases from 0.22 to 0.42. While the prevailing period changes between 0.06 and 0.29, the spectral acceleration value changes between 0.8 and 1. As with other sections, the results of the Plaxis is quite large values.

At 5E point at the bottom of the valley, there is bedrock and a fill layer of 5 m on this bedrock. In the depth analysis, it is seen that the EERA results are lower. While the acceleration does not change greatly where the bedrock is situated, it rapidly increases with the beginning of the fill layer. The results of the two-dimensional analyses do not change. In the spectral acceleration-period graph, the results of the Deepsoil analysis reach a peak value of 2.5 and the prevailing period is quite narrow. The reason is

that the thickness of fill layer is thin and as the layer thickness increases, the effect of earthquake is higher and the period is extended.

The 5F point is situated almost in the middle of a slope which consists of a clayey layer of 25 m and a fill layer of 3 m. It is seen that the acceleration changes by depth much more when compared to the 5E point. The reason for this could be the thick clayey layer. The result of two-dimensional analysis increases from 0.33 to 0.40 from the bedrock to the surface. The spectral acceleration-period graph takes the biggest spectral acceleration value between the time interval of 0.14–0.36 and is seen as a prevailing time interval. It is seen that the thick clayey layer of about 25 m causes the earthquake force to be more effective and that the repetition period increases as there is no repetition frequency although the peak value of the fill layer with a thickness of 5 m at the 5E point is higher.

4.3 Effect of surface topography on soil behavior

Section 5-5' was selected in order to examine the effect of surface topography on the analysis results. A simplified model in which the surface and material borders are assumed to be flat was formed (Fig. 20) and the surface acceleration values were obtained from the analyses carried out (Fig. 21).

Figure 21 shows that the acceleration values at the 5D point that is actually a valley are very close to each other in the one-dimensional analyses and the value is 0.6 but the result of one-dimensional analyses differ being 0.58 for the Deepsoil nonlinear and EERA models, while increasing to 0.66 for the Deepsoil equivalent linear analysis. Examining the result of the two-dimensional analysis, this value which was 0.42 increased to 0.57 in the flattened case. The results of the one-dimensional analyses at the 5E point exhibit similar behaviors and reach the bottom level but the results of the Deepsoil equivalent linear (EL) and Deepsoil non linear (NL) analyses continue to flatten. As the result of two-dimensional analysis the value is 0.46, increasing to 0.69 in the flattened case thus, it can be seen that when the surface flattens, the acceleration value increases. At the 5G point, as the acceleration value increases from 0.48 to

[Title Page](#)

[Abstract](#)

[Introduction](#)

[Conclusions](#)

[References](#)

[Tables](#)

[Figures](#)

◀

▶

[Back](#)

[Close](#)

[Full Screen / Esc](#)

[Printer-friendly Version](#)

[Interactive Discussion](#)

0.58 in the two-dimensional analysis, the results of one-dimensional analyses make the graphs horizontal and the values range from 0.40 to 0.60. In the real topography, as the graph of one-dimensional analyses results decline, its value changes from 0.48 to 0.64. At the 5H point, as the results of the one-dimensional analyses reach the bottom value, the value changes from 0.37 to 0.47 and it is 0.48 in the two-dimensional analyses. In the flattened section, the one-dimensional analysis results of the same point are parallel to each other and have a ascending tendency and their values change from 0.47 to 0.59. The one-dimensional analysis results reach the peak level at the 5I point at the bottom of the second valley and their values change from 0.53 to 0.63; while the value is 0.47 in the two-dimensional analyses, they increase to 0.54 in case of flattening. At the 5J point which is the final hilly part, the one-dimensional analysis results give almost the same lowest values and are around 0.44. When examining these values in case of flattening, they change from 0.40 to 0.44 in the one-dimensional analysis, they increase to 0.60 in the two-dimensional analysis.

Considering the results, it is observed that the surface topography has an influence on, and changes the acceleration value. Moreover, when the field topography becomes flat, the acceleration values can be said to generally increase in the one and two-dimensional analyses.

References

20 Ansal, A. M., Yıldırım, H., and Erken, A.: Cyclic Stress–Strain–Pore Pressure Behaviour of Soils, Proc. Of Int. Symposium on 70 Years of Soil Mechanics, 2–7 April 1995, Istanbul, Vol. 2, 43–71, 1995.

25 Bardet, J. P., Ichii, K., and Lin, C. H.: EERA: A Computer Program for Equivalent-Linear Earthquake Response Analyses of Layered soil Deposits, University of Southern California, Los Angeles, 2000.

Hasal, M. E.: The Effect of Topographical Irregularities on Soil Amplification, Ms. thesis, Istanbul Technical University, İstanbul, 2009 (in Turkish).

[Title Page](#)

[Abstract](#) [Introduction](#)

[Conclusions](#) [References](#)

[Tables](#) [Figures](#)

◀

▶

◀

▶

Back

Close

Full Screen / Esc

[Printer-friendly Version](#)

[Interactive Discussion](#)

Topographic irregularities and 2-D effects on the surface

L. Yılmazoğlu and
G. Ç. İnce

Hashash, Y. M. A., Groholski, D. R., Phillips, C. A., and Park, D.: DEEPSOIL V3.7 beta, Users Manual and Tutorial, 88 pp., 2009.

Idriss, I. M.: Response of soft soil sites during earthquakes, Proceedings of the Symposium to Honor Professor Harry Bolton Seed, Berkeley, California, USA, II, 273–289, 1990.

5 İnce, G., Ç., Özaydın, K., Yıldırım, M., and Özener, P.: Geological and geotechnical structure of historical peninsula (İstanbul) and its seismic microzonation, Bull. Eng. Geol. Environ., 67, 41–51, doi:10.1007/s10064-007-0099-9, 2008.

İnce, G. Ç.: Probabilistic seismic hazard assessment of the historical peninsula of Istanbul, Nat. Hazards Earth Syst. Sci., 12, 3483–3493, doi:10.5194/nhess-12-3483-2012, 2012.

10 Kale, P.: Investigation of the effect of local soil condition with one and two dimensional analyses, Ms. thesis, Yıldız Technical University, İstanbul, 2008 (in Turkish).

Papageorgiou, A., Halldorsson, B., and Dong, G.: TARSCTHS: target acceleration spectra compatible time histories, Dept. of Civil, Structural and Environmental Engrg., University of Buffalo, North Campus, Buffalo, NY, 2000.

15 Plaxis: Finite Element Code for soil and rock analyses, Version 8, edited by: Brinkgreve, R. B. J. and Vermeer, P. A., A.A. Balkema, Rotterdam, Brookfield, 2005.

Schnabel, P. B., Lysmer, J., and Seed, H. B.: SHAKE: a Computer Program for Earthquake Response Analysis of Horizontally Layered Sites, Report EERC 72-12, Earthquake Engineering Research Center, University of California, Berkeley, 1972.

20 Seed, H. B. and Idriss, I. M.: Soil Moduli and Damping Factors for Dynamic Response Analyse, Report No:EERC 70-10, EERC, University of California, Berkley, USA, 1970.

Vucetic, M. and Dobry, R.: Effect of soil plasticity on cyclic respons, American society of Civil Engineering, J. Geotech. Eng., 117, 89–107, 1991.

25 Yıldırım, M. and Savaşkan, E.: A New Approach to the Stratigraphy of the Tertiary Sedimentary Formations in Istanbul and Their Engineering Properties, Proceedings of National Symposium on İstanbul's Geology, 20–21 December, Kadir Has University, Cibali-İstanbul, 87–102, 2003.

Title Page

Abstract

Introduction

Conclusions

References

Tables

Figures

◀

▶

◀

▶

Back

Close

Full Screen / Esc

Printer-friendly Version

Interactive Discussion

Topographic irregularities and 2-D effects on the surface

L. Yılmazoğlu and
G. Ç. İnce

[Title Page](#)

[Abstract](#) [Introduction](#)

[Conclusions](#) [References](#)

[Tables](#) [Figures](#)



[Full Screen / Esc](#)

[Printer-friendly Version](#)

[Interactive Discussion](#)

Table 1. Selected points and their locations.

Point	Section number	Location	Point	Section number	Location
1A	1	Plain	4A	4	Heel of hillside
1B	1	Top of hillside	4B	4	Heel of hillside
1C	1	Skirt of hillside	4C	4	Top of hillside
1D	1	Top of hillside	4D	4	Top of hillside
1E	1	Skirt of hillside	4E	4	Skirt of hillside
1F	1	Plain	4F	4	Heel of hillside
2A	2	Heel of hillside	4G	4	Top of hillside
2B	2	Plain	4H	4	Top of hillside
2C	2	The heel of hillside	4I	4	Top of hillside
2D	2	Plain	4J	4	Plain
2E	2	Skirt of hillside	4K	4	Top of hillside
2F	2	Plain	5A	5	Plain
3A	3	Heel of hillside	5B	5	Top of hillside
3B	3	Top of hillside	5C	5	Plain
3C	3	Plain	5D	5	Skirt of hillside
3D	3	Top of hillside	5E	5	The heel of hillside
3E	3	Skirt of hillside	5F	5	Top of hillside
3F	3	Skirt of hillside	5G	5	Top of hillside
3G	3	Skirt of hillside	5H	5	Plain
3H	3	Plain	5I	5	Heel of hillside
			5J	5	Top of hillside
			5K	5	Plain

Topographic irregularities and 2-D effects on the surface

L. Yılmazoğlu and
G. Ç. İnce

[Title Page](#)

[Abstract](#)

[Introduction](#)

[Conclusions](#)

[References](#)

[Tables](#)

[Figures](#)

[◀](#)

[▶](#)

[◀](#)

[▶](#)

[Back](#)

[Close](#)

[Full Screen / Esc](#)

[Printer-friendly Version](#)

[Interactive Discussion](#)

Table 2. Selected G/G_{\max} and damping relations for the formations.

FORMATION	γ_n (kN m^{-3})	Material	Strain-dependent relationships	$V_{(\min-\max)}$ (m s^{-1})
Fill 1(Haliç deposits)	15.5	Mat 1	G/G_{\max} : Vucetic and Dobry (1991), $Ip = 25\%$ Damping ratio: Vucetic and Dobry (1991), $Ip = 25\%$	78–182
Fill1(artificial fill)	18	Mat 1	G/G_{\max} : Vucetic and Dobry (1991), $Ip = 25\%$ Söñüm oranı: Vucetic and Dobry (1991), $Ip = 25\%$	204–358
Fill 2(Alluvial)	18	Mat 2	G/G_{\max} : Vucetic and Dobry (1991), $Ip = 30\%$ Söñüm oranı: Vucetic and Dobry (1991), $Ip = 30\%$	140–340
Bakırköy Clay	19	Mat 3	G/G_{\max} : Vucetic and Dobry (1991), $Ip = 45\%$ Söñüm oranı: Vucetic and Dobry (1991), $Ip = 45\%$	280–385
Bakırköy Limestone and Gürpınar Limestone	24	Mat 4	Attenuation of rock average and damping in rock, Idriss (1990)	314–473
Gürpınar Clay	20	Mat 5	G/G_{\max} : Vucetic and Dobry (1991), $Ip = 40\%$ Damping ratio: Vucetic and Dobry (1991), $Ip = 40\%$	101–443
Çukurçeşme and Gürpi- nar Sand	20	Mat 6	G/G_{\max} : Seed and Idriss (1970), upper range Damping ratio: (Idriss, 1990)	119–473
Gürpınar Base (sandy gravel)	21	Mat 7	G/G_{\max} : Seed and Idriss (1970), upper range Damping ratio: Seed and Idriss (1970), average	222–473
Trakya limestone (bedrock)	25	–	Idriss (1990)	700

* V_{\min} is a value at the upper levels of the layer and V_{\max} is the value at the lower levels of the layer.

Topographic irregularities and 2-D effects on the surface

L. Yılmazoğlu and
G. Ç. İnce

Table 3. The material parameters in used Plaxis for all formations.

Formations	Material Model	γ_{dry} (kN m ⁻³)	$\gamma_{\text{saturated}}$ (kN m ⁻³)	c (kN m ⁻²)	φ (°)	E50ref (kPa)	Eurref (kPa)	Eref (kPa)	Vs* (m s ⁻¹)
Artificial Fill Haliç Sediments	Hardening Soil	18	19	1	25	1.126×10^{05}	3.885×10^{05}	–	–
	Soft Soil	12	16.5	1	14	–	–	–	–
Alluvial fill	Mohr–Coulomb	13.30	18	1	25	–	–	2.349×10^{05}	258
Bakırköy Clay Bakırköy and Gürpınar Limestone	Hardening Soil	21	22	12	25	9.257×10^{05}	3.124×10^{06}	–	–
Gürpınar Clay	Hardening Soil	21	22	12	25	9.257×10^{05}	3.124×10^{06}	–	–
Gürpınar Base Gürpınar and Çukurçeşme sand	Hardening Soil	20	21	1	25	7.052×10^{05}	2.080×10^{06}	–	–
Bedrock	Mohr–Coulomb	21	21	1	35	6.022×10^{05}	1.298×10^{06}	–	–
Çukurçeşme sand	Linear elastic	19	20	1	30	–	–	6.14×10^{05}	349
Bedrock	Linear elastic	26	28	1	36	9.80×10^{05}	2.940×10^{06}	3.12×10^{06}	700

Table 4. α and β values at selected points for all sections.

Point	Section number	ω_1 and ω_2	α	β
1A	1	1-3	0.075	0.025
1B	1	1-8	0.089	0.0111
1C	1	1-5	0.0833	0.0167
1D	1	1-5	0.0833	0.0167
1E	1	1-5	0.0833	0.0167
1F	1	1-3	0.075	0.025
2A	2	1-5	0.0833	0.0167
2B	2	1-5	0.0833	0.0167
2C	2	1-8	0.089	0.0111
2D	2	1-5	0.0833	0.0167
2E	2	1-5	0.0833	0.0167
2F	2	1-3	0.075	0.025
3A	3	1-8	0.0890	0.0111
3B	3	1-8	0.0890	0.0111
3C	3	1-8	0.0890	0.0111
3D	3	1-8	0.0890	0.0111
3E	3	1-5	0.0833	0.0167
3F	3	1-5	0.0833	0.0167
3G	3	1-8	0.0890	0.0111
3H	3	1-8	0.0890	0.0111
4A	4	1-8	0.0890	0.0111
4B	4	1-8	0.0890	0.0111
4C	4	1-8	0.0890	0.0111
4D	4	1-8	0.0890	0.0111
4E	4	1-8	0.0890	0.0111
4F	4	1-3	0.075	0.025
4G	4	1-3	0.075	0.025
4H	4	1-8	0.0890	0.0111
4I	4	1-8	0.0890	0.0111
4J	4	1-8	0.0890	0.0111
4K	4	1-3	0.075	0.025
5A	5	1-8	0.0890	0.0111
5B	5	1-8	0.0890	0.0111
5C	5	1-8	0.0890	0.0111
5D	5	1-8	0.0890	0.0111
5E	5	1-8	0.0890	0.0111
5F	5	1-5	0.0833	0.0167
5G	5	1-8	0.0890	0.0111
5H	5	1-5	0.0833	0.0167
5I	5	1-8	0.0890	0.0111
5J	5	1-8	0.0890	0.0111
5K	5	1-8	0.0890	0.0111

Topographic irregularities and 2-D effects on the surface

L. Yılmazoğlu and
G. Ç. İnce

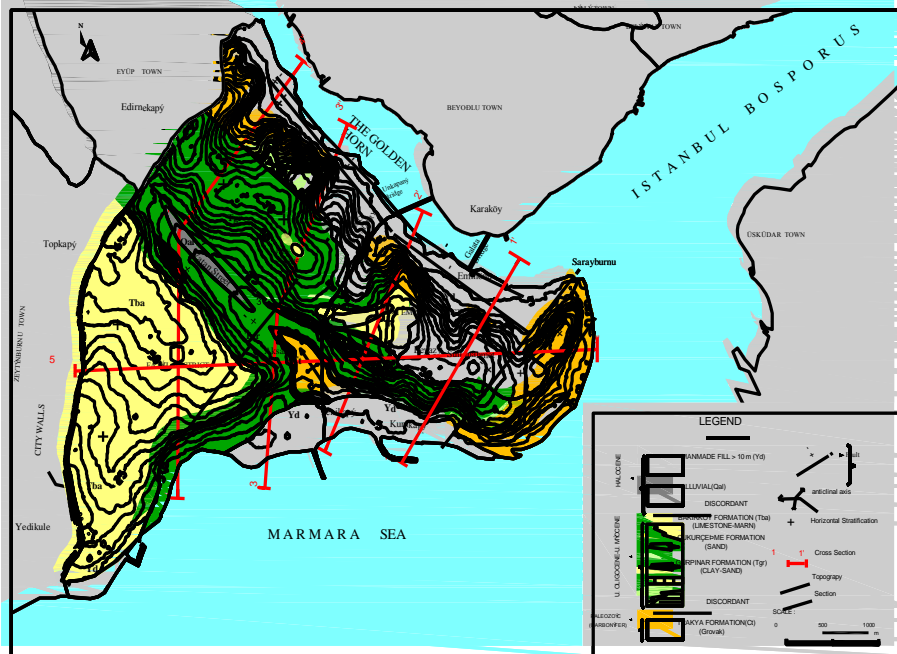


Fig. 1. Geological map containing the five cross-sections used in the analysis.

Topographic irregularities and 2-D effects on the surface

L. Yılmazoğlu and
G. Ç. İnce

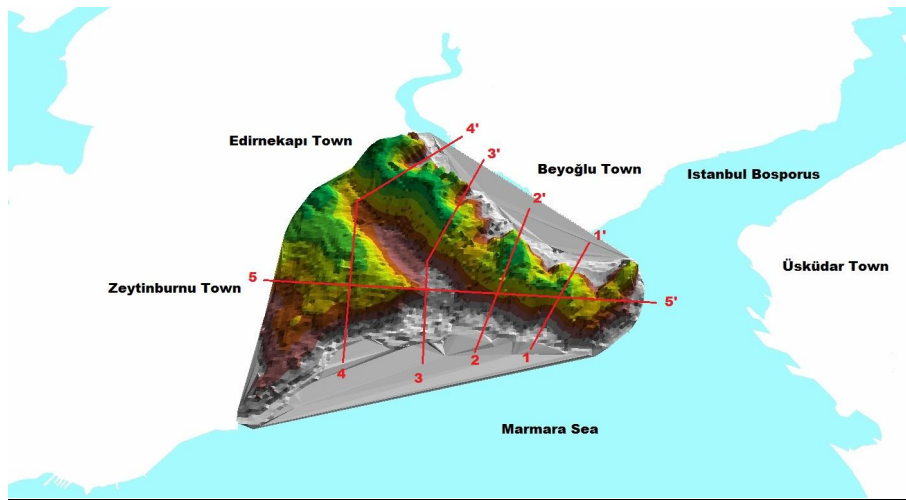


Fig. 2. Three-dimensional image of the 5 sections analysed in the study.

- [Title Page](#)
- [Abstract](#) [Introduction](#)
- [Conclusions](#) [References](#)
- [Tables](#) [Figures](#)
- [◀](#) [▶](#)
- [◀](#) [▶](#)
- [Back](#) [Close](#)
- [Full Screen / Esc](#)
- [Printer-friendly Version](#)
- [Interactive Discussion](#)

Topographic irregularities and 2-D effects on the surface

L. Yılmazoğlu and
G. Ç. İnce

Fig. 3. The location of the points on the 1-1' cross section where the 1-D and 2-D analyses were performed (Ince et al., 2008).

Title Page

Abstract

Introduction

Conclusions

Figures

1

▶

Back

Close

Full Screen / Esc

[Printer-friendly Version](#)

Interactive Discussion

Topographic irregularities and 2-D effects on the surface

L. Yılmazoğlu and
G. Ç. İnce

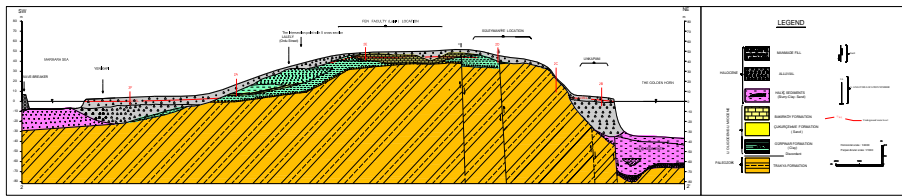


Fig. 4. The location of the points on the 2-2' cross section where the 1-D and 2-D analyses were performed (İnce et al., 2008).

[Title Page](#)

[Abstract](#)

[Introduction](#)

[Conclusions](#)

[References](#)

[Tables](#)

[Figures](#)

◀

▶

◀

▶

[Back](#)

[Close](#)

[Full Screen / Esc](#)

[Printer-friendly Version](#)

[Interactive Discussion](#)

**Topographic
irregularities and 2-D
effects on the surface**

L. Yılmazoğlu and
G. Ç. İnce

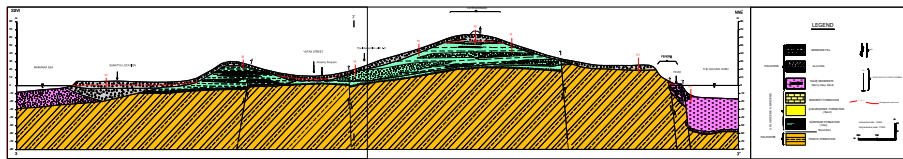


Fig. 5. The location of the points on the 3-3' cross section where the 1-D and 2-D analyses were performed (İnce et al., 2008).

[Title Page](#)[Abstract](#)[Introduction](#)[Conclusions](#)[References](#)[Tables](#)[Figures](#)[◀](#)[▶](#)[◀](#)[▶](#)[Back](#)[Close](#)[Full Screen / Esc](#)[Printer-friendly Version](#)[Interactive Discussion](#)

**Topographic
irregularities and 2-D
effects on the surface**

L. Yılmazoğlu and
G. Ç. İnce

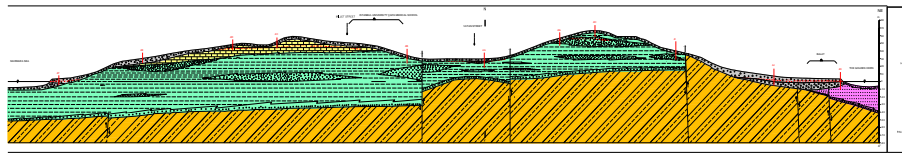


Fig. 6. The location of the points on the 4-4' cross section where the 1-D and 2-D analyses were performed (İnce et al., 2008).

[Title Page](#)[Abstract](#)[Introduction](#)[Conclusions](#)[References](#)[Tables](#)[Figures](#)[◀](#)[▶](#)[◀](#)[▶](#)[Back](#)[Close](#)[Full Screen / Esc](#)[Printer-friendly Version](#)[Interactive Discussion](#)

**Topographic
irregularities and 2-D
effects on the surface**

L. Yılmazoğlu and
G. Ç. İnce

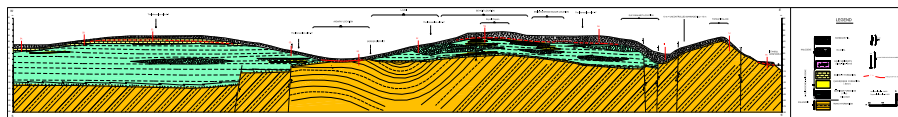


Fig. 7. The location of the points on the 5-5' cross section where the 1-D and 2-D analyses were performed (İnce et al., 2008).

[Title Page](#)[Abstract](#)[Introduction](#)[Conclusions](#)[References](#)[Tables](#)[Figures](#)[◀](#)[▶](#)[◀](#)[▶](#)[Back](#)[Close](#)[Full Screen / Esc](#)[Printer-friendly Version](#)[Interactive Discussion](#)

**Topographic
irregularities and 2-D
effects on the surface**

L. Yılmazoğlu and
G. Ç. İnce

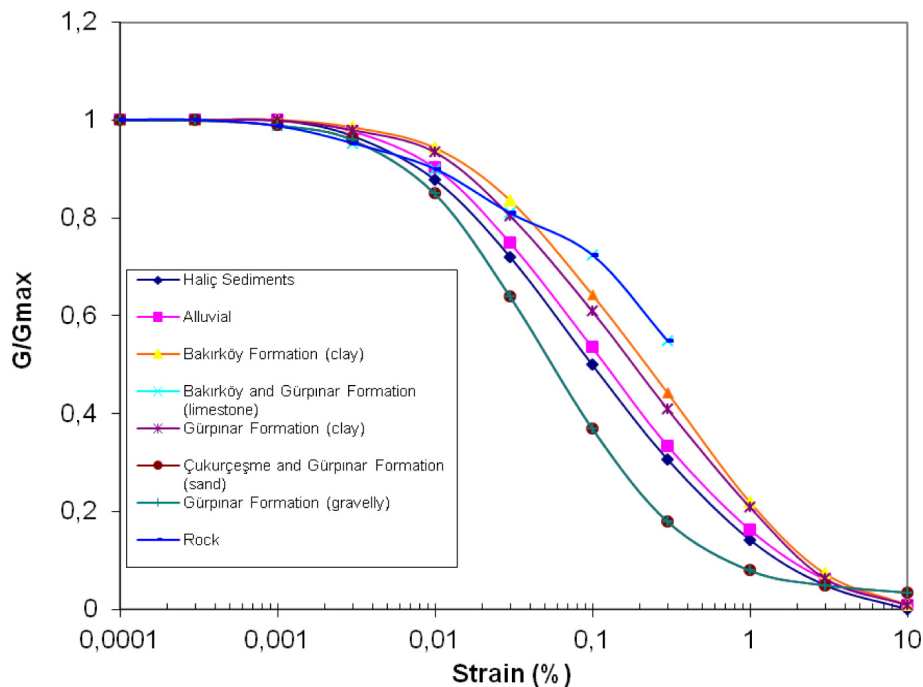


Fig. 8. G/G_{\max} and shear strain relationships for all formations.

**Topographic
irregularities and 2-D
effects on the surface**

L. Yılmazoğlu and
G. Ç. İnce

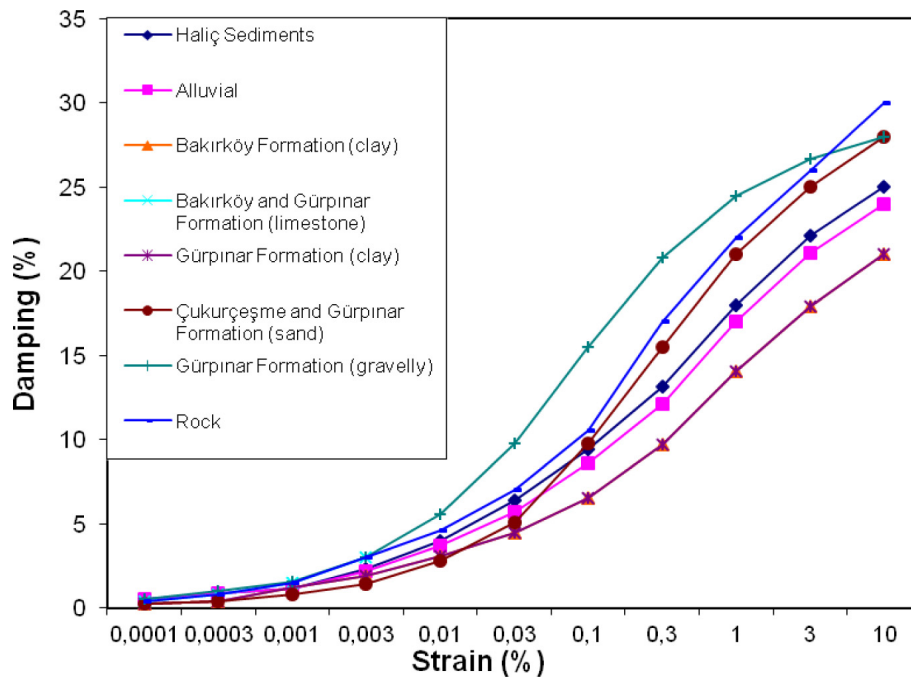


Fig. 9. Damping ratio and shear strain relationships for all formations.

- [Title Page](#)
- [Abstract](#) [Introduction](#)
- [Conclusions](#) [References](#)
- [Tables](#) [Figures](#)
- [◀](#) [▶](#)
- [◀](#) [▶](#)
- [Back](#) [Close](#)
- [Full Screen / Esc](#)
- [Printer-friendly Version](#)
- [Interactive Discussion](#)

**Topographic
irregularities and 2-D
effects on the surface**

L. Yılmazoğlu and
G. Ç. İnce

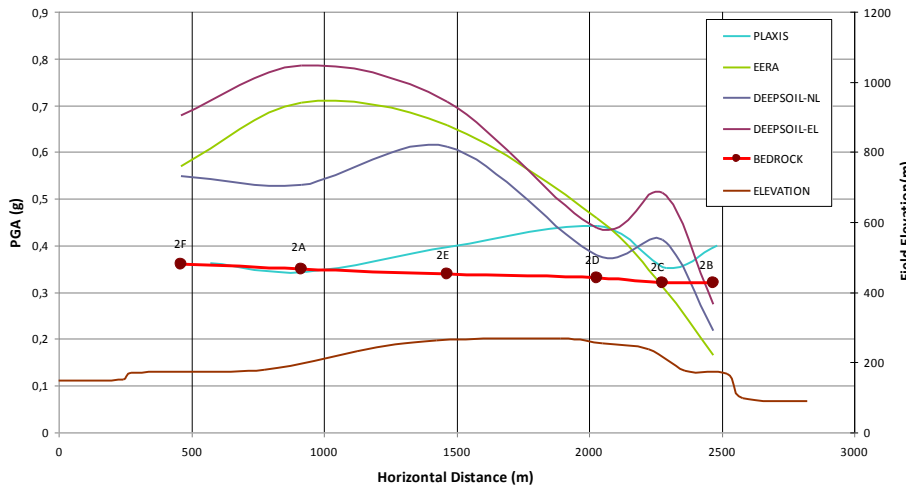


Fig. 11. Change in the peak ground acceleration on the surface for 2-2' section.

**Topographic
irregularities and 2-D
effects on the surface**

L. Yılmazoğlu and
G. Ç. İnce

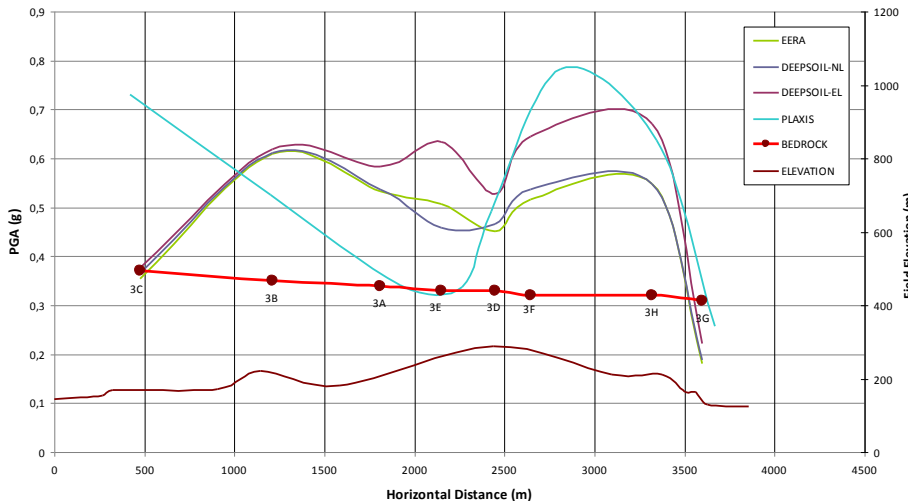


Fig. 12. Change in the peak ground acceleration on the surface for the 3-3' section.

- [Title Page](#)
- [Abstract](#) [Introduction](#)
- [Conclusions](#) [References](#)
- [Tables](#) [Figures](#)
- [◀](#) [▶](#)
- [◀](#) [▶](#)
- [Back](#) [Close](#)
- [Full Screen / Esc](#)
- [Printer-friendly Version](#)
- [Interactive Discussion](#)

**Topographic
irregularities and 2-D
effects on the surface**

L. Yılmazoğlu and
G. Ç. İnce

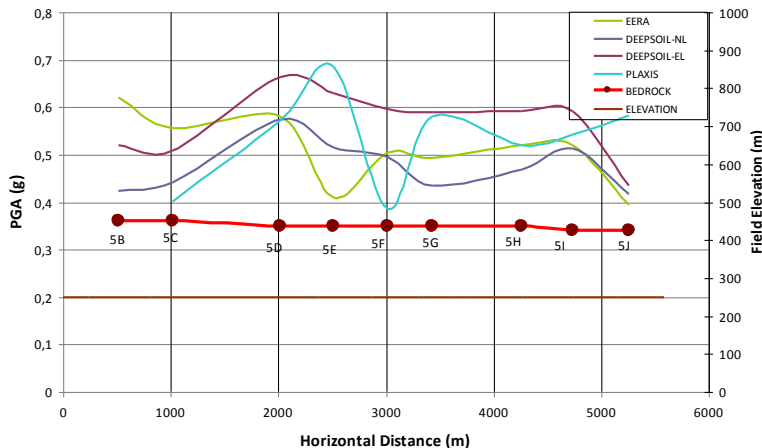


Fig. 15. 1-1' section; maximum acceleration-depth and spectral acceleration-period graphic for the points selected.

[Title Page](#)[Abstract](#)[Introduction](#)[Conclusions](#)[References](#)[Tables](#)[Figures](#)[◀](#)[▶](#)[◀](#)[▶](#)[Back](#)[Close](#)[Full Screen / Esc](#)[Printer-friendly Version](#)[Interactive Discussion](#)

Topographic irregularities and 2-D effects on the surface

L. Yılmazoğlu and
G. Ç. İnce

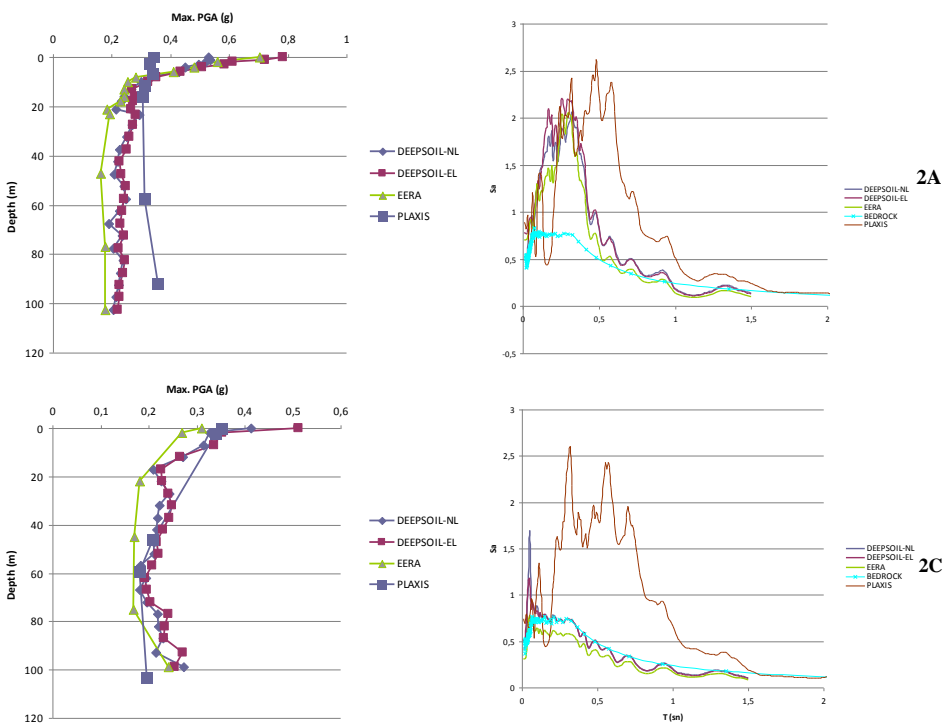


Fig. 16. 2-2' section; maximum acceleration-depth and spectral acceleration-period graph for the selected points.

Topographic irregularities and 2-D effects on the surface

L. Yılmazoğlu and
G. Ç. İnce

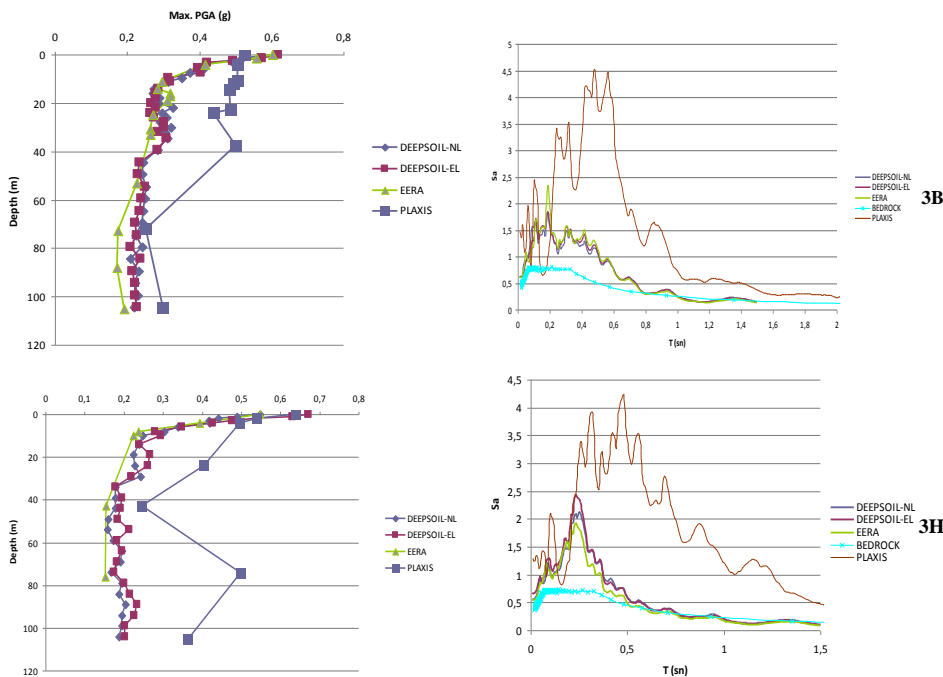


Fig. 17. 3-3' section; maximum acceleration-depth and spectral acceleration-period graph for the selected points.

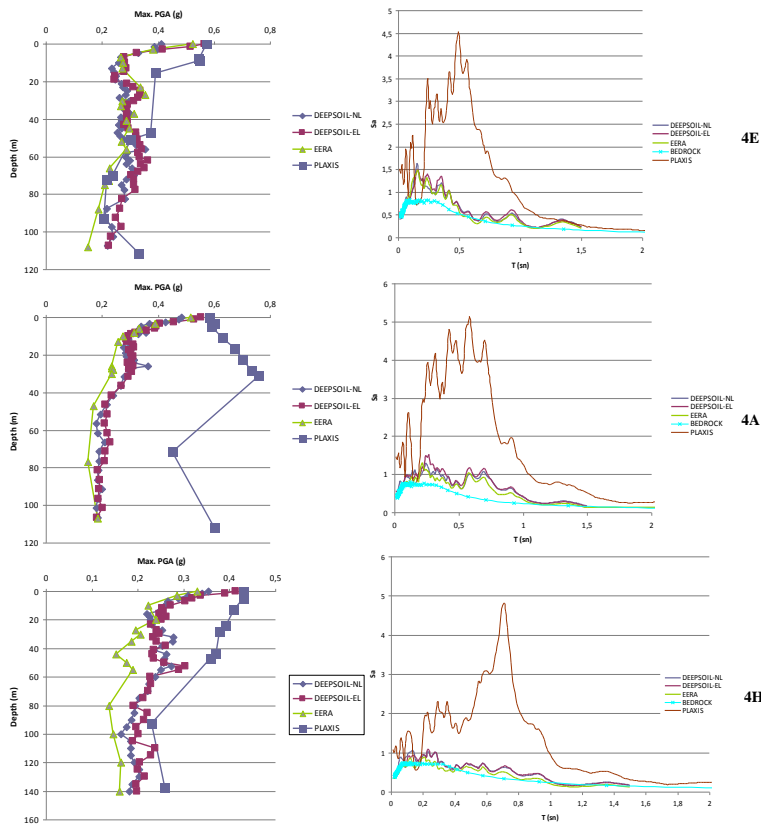


Fig. 18. 4-4' section; maximum acceleration-depth and spectral acceleration-period graph for the selected points.

Topographic irregularities and 2-D effects on the surface

L. Yılmazoğlu and
G. Ç. İnce

Title Page

Abstract

Introduction

Conclusion

References

Fig. 19. 5-5' section; maximum acceleration-depth and spectral acceleration-period graphic for the selected points.

Topographic irregularities and 2-D effects on the surface

L. Yılmazoğlu and
G. Ç. İnce

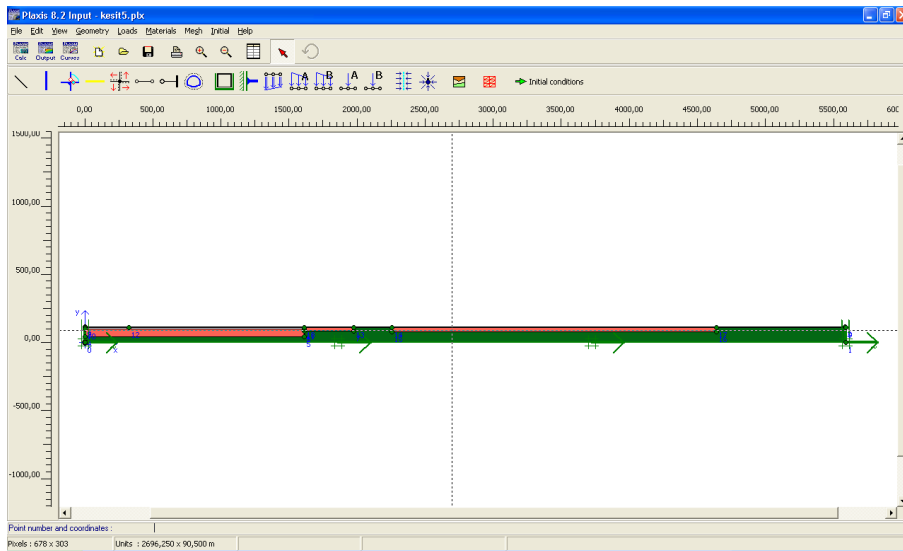


Fig. 20. For the 5-5' section, a simplified model in which the surface and material borders are assumed to be flat.

Title Page

Abstract

Introduction

Conclusions

References

Tables

Figures

◀

▶

◀

▶

Back

Close

Full Screen / Esc

**Topographic
irregularities and 2-D
effects on the surface**

L. Yılmazoğlu and
G. Ç. İnce

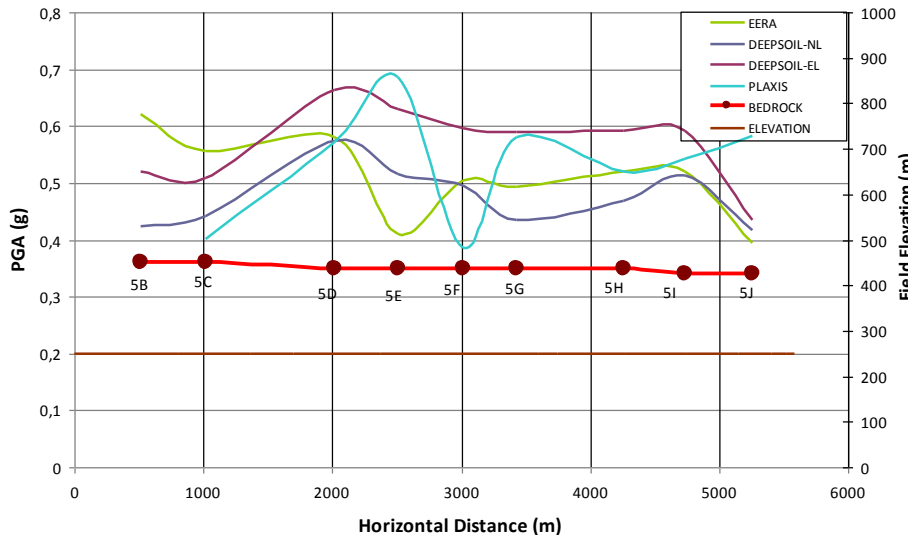
[Title Page](#)[Abstract](#)[Introduction](#)[Conclusions](#)[References](#)[Tables](#)[Figures](#)[◀](#)[▶](#)[◀](#)
[Back](#)[▶](#)
[Close](#)[Full Screen / Esc](#)[Printer-friendly Version](#)[Interactive Discussion](#)

Fig. 21. Change of maximum acceleration by depth for 5 points chosen for the section.